

The impact of successive earthquakes on the seismic damage of multistorey 3D R/C buildings

Konstantinos Kostinakis^{1a} and Konstantinos Morfidis^{*2}

¹Department of Civil Engineering, Aristotle University of Thessaloniki, Aristotle University campus, 54124, Thessaloniki, Greece

²Earthquake Planning and Protection Organization (EPPO-ITSAK), Dasyliou Str., 55535, Thessaloniki, Greece

(Received November 12, 2015, Revised November 8, 2016, Accepted November 8, 2016)

Abstract. Historical earthquakes have shown that successive seismic events may occur in regions of high seismicity. Such a sequence of earthquakes has the potential to increase the damage level of the structures, since any rehabilitation between the successive ground motions is practically impossible due to lack of time. Few studies about this issue can be found in literature, most of which focused their attention on the seismic response of SDOF systems or planar frame structures. The aim of the present study is to examine the impact of seismic sequences on the damage level of 3D multistorey R/C buildings with various structural systems. For the purposes of the above investigation a comprehensive assessment is conducted using three double-symmetric and three asymmetric in plan medium-rise R/C buildings, which are designed on the basis of the current seismic codes. The buildings are analyzed by nonlinear time response analysis using 80 bidirectional seismic sequences. In order to account for the variable orientation of the seismic motion, the two horizontal accelerograms of each earthquake record are applied along horizontal orthogonal axes forming 12 different angles with the structural axes. The assessment of the results revealed that successive ground motions can lead to significant increase of the structural damage compared to the damage caused by the corresponding single seismic events. Furthermore, the incident angle can radically alter the successive earthquake phenomenon depending on the special characteristics of the structure, the number of the sequential earthquakes, as well as the distance of the record from the fault.

Keywords: repeated earthquakes; seismic sequences; reinforced concrete buildings; seismic incident angle; seismic damage; bidirectional excitation

1. Introduction

Structures located in high seismic risk areas often experience seismic sequences characterized by the repetition of ground motions with high magnitude occurring at short intervals of time one after the other. The seismic sequences consist of a main seismic event accompanied by foreshocks or aftershocks with comparable or even higher magnitude. Such kind of successive earthquakes have been observed in several hazard-prone areas, such as Greece (1986, 1988, 2014), Italy (Friuli 1976, Umbria-Marche 1997, L'Aquila 2009), Turkey (1992, 1999, 2011), California (Mammoth Lakes 1980, Whittier Narrows 1987, Northridge 1994), Mexico (1985, 1993, 1994), Chile (2010) and New Zealand (2010, 2011). In the case of successive earthquakes there is no time for the structures already damaged by the first earthquake ground motion to be repaired before the occurrence of the seismic events following, so successive earthquakes with significant magnitude may increase structural damage or even drive the building to become completely unusable at the end of the seismic sequence (e.g., Priestley 1988, Elnashai *et al.* 2009,

Augenti and Parisi 2010, Jing *et al.* 2011). Despite the possible destructive effects of the successive strong motions, the design strategies introduced by the modern seismic code provisions (e.g., EN1998-1 2004, FEMA-356 2000, ASCE/SEI 41-06 2008) are based on single earthquakes ignoring the impact of foreshock-mainshock-aftershock sequence-type ground motions. These procedures may lead to significant underestimation of seismic response and structural damage levels.

The influence of the sequential earthquakes on the seismic response of single-degree-of-freedom (SDOF) structural systems with various hysteretic models has been extensively investigated by numerous researchers (e.g., Amadio *et al.* 2003, Hatzigeorgiou and Beskos 2009, Hatzigeorgiou 2010a, Sarno 2013, Zhai *et al.* 2013). The general conclusion of these studies was that the structural response evaluated in terms of maximum inelastic displacement, maximum acceleration, dissipated energy, peak ductility demands or damage indices may be completely different from the seismic response produced when the SDOF system is subjected to a single earthquake record. In particular, the seismic damage levels were higher for the seismic sequences. Moreover, it was shown that seismic sequences necessitate smaller behavior factors in comparison with the single ground motions.

Similar conclusions were derived by researchers who studied multiple-degree-of-freedom (MDOF) systems. For example, in a preliminary study (Fragiacomo *et al.* 2004),

*Corresponding author, Assistant Researcher
E-mail: konmorf@gmail.com

^aPost-Doc Researcher

examined the influence of successive earthquakes on the nonlinear response of planar steel frames and showed that the repetition of medium-high intensity earthquake ground motions at short time one after the other produces an accumulation of damage, which should be considered in earthquake-prone regions. Later, Hatzigeorgiou and Liolios (2010) conducted an extensive parapetric study on the inelastic response of eight R/C planar frames which were subjected to sequential ground motions. It was found that the successive earthquakes have a significant effect on the seismic response and, hence, on the design of the R/C frames. Another investigation was carried out by Ruiz-Garcia and Negrete-Manriquez (2011), who investigated the impact of the successive earthquakes on the peak and residual drift demands of three steel frame models. They showed that artificial seismic sequences, unlike real mainshock-aftershock seismic events, can significantly increase the drift demands. In another study, Efraimiadou *et al.* (2013) examined the effects of collision between adjacent R/C buildings under successive earthquakes. For the needs of the investigation four planar frames and nine different pairs of adjacent R/C structures were subjected to five real seismic sequences. The results revealed that the seismic sequences were detrimental in comparison with the single seismic events. More recently, Ruiz-Garcia *et al.* (2014) investigated the impact of soft-soil artificial seismic sequences on the structural response of R/C frames and found that the relationship of the damaged period of the building to the predominant period of the aftershock significantly influences the seismic response. In another research (Shin *et al.* 2014), the seismic assessment of a damaged piloti-type R/C structure under repeated earthquake ground motions was carried out and a framework to evaluate the effectiveness of retrofitting was proposed.

It must be noted that all the above investigations were restricted to planar R/C or steel frames, thus accounting for only one component of the strong motion records. Modern seismic codes (e.g., UBC 1997, FEMA-356 2000, NEHRP 2003, EN1998-1 2004, ASCE/SEI 41-06 2008) suggest that structures shall be designed for the two horizontal translational components of ground motion (in the majority of buildings the vertical component can be neglected). In this case 3-dimensional models are used in order to efficiently simulate the real structures and to adequately capture their seismic response. To the best of the authors' knowledge, only two studies exist that deal with the nonlinear response of 3D buildings under bidirectional seismic sequences. The first study (Zahid *et al.* 2012) investigated the effects of successive earthquakes on the response of high-rise R/C buildings. For this purpose, five 18-storey generic R/C models with five different behavior factors were subjected to 40 artificial seismic sequences consisting of randomly combined near-fault single ground motions. The displacement and the storey ductility demand were used as the damage indicators for the R/C models. It was found that the influence of the repeated near-fault earthquakes on the structural response can be significant compared to the damage caused by the corresponding single seismic events. The second study (Faisal *et al.* 2013)

focused on the influence of successive earthquakes on the maximum storey ductility demands of R/C frames. For this purpose, sixty moment-resisting symmetric frame systems with single-bay configuration were subjected to numerous artificial seismic sequences. The research revealed that repeated earthquakes significantly increase the storey ductility demand of inelastic concrete frames. On average, relative increment of maximum storey ductility demand was experienced 1.4 and 1.3 times when double and triple events of repeated earthquakes were induced, respectively. However, as the authors recognized, the latter numerical study was neither exhaustive nor conclusive, since they examined only symmetric single-bay buildings without walls and structural eccentricity.

Another critical issue that must be examined is the influence of the incident angle on the inelastic response of buildings under successive earthquake ground motions. As it has been shown by many researchers, even for quite simple buildings, the angle of seismic incidence can radically alter the analysis results in terms of the elastic response and design of structures (Athanatopoulou 2005, Athanatopoulou *et al.* 2005, Kostinakis *et al.* 2010, 2012), as well as of the inelastic response and damage level (Rigato and Medina 2007, Lagaros 2010, Lucchini *et al.* 2011, Kostinakis *et al.* 2013, Fontara *et al.* 2015). Moreover, the distance of the record from the fault is a factor which can also significantly influence the basic characteristics of the seismic excitation (e.g., frequency content, peak acceleration) and so it can affect the impact of the seismic sequences on the structural response as well as the damage level of the building (e.g., Alavi and Krawinkler 2001, Kalkan and Kunnath 2006). Thus, the need of a study dealing with the effects of successive earthquakes on the seismic response of 3D structures with different structural systems taking into account all the above issues is apparent.

The objective of the present paper is to investigate the influence of seismic sequences on the damage response of 3D multistorey buildings with various structural systems. To accomplish this purpose six medium-rise R/C buildings are studied. All buildings have five stories and their structural systems consist of vertical elements in two perpendicular directions. The buildings, which have been designed on the basis of EN1998-1 (2004) and EN1992-1-1 (2004) provisions, are analyzed by means of Nonlinear Time Response Analysis (NTRA) for 40 single ground motions (20 far-fault and 20 near-fault records) as well as for 80 bidirectional seismic sequences. Moreover, in order to account for the influence of the incident angle on the structural response, the two horizontal accelerograms of each ground motion are applied along horizontal orthogonal axes forming an angle $\theta=0^\circ, 30^\circ, 60^\circ, \dots, 330^\circ$ with the structural axes. For the evaluation of the expected structural damage state of each building the Maximum Interstorey Drift Ratio (MIDR) is determined. The results show that the MIDR of the buildings subjected to sequential earthquakes can be significantly larger (up to 138.1%) than the MIDR produced by the corresponding single seismic events. Furthermore, the incident angle can radically alter the successive earthquake phenomenon depending on the special characteristics of the structure, the number of the

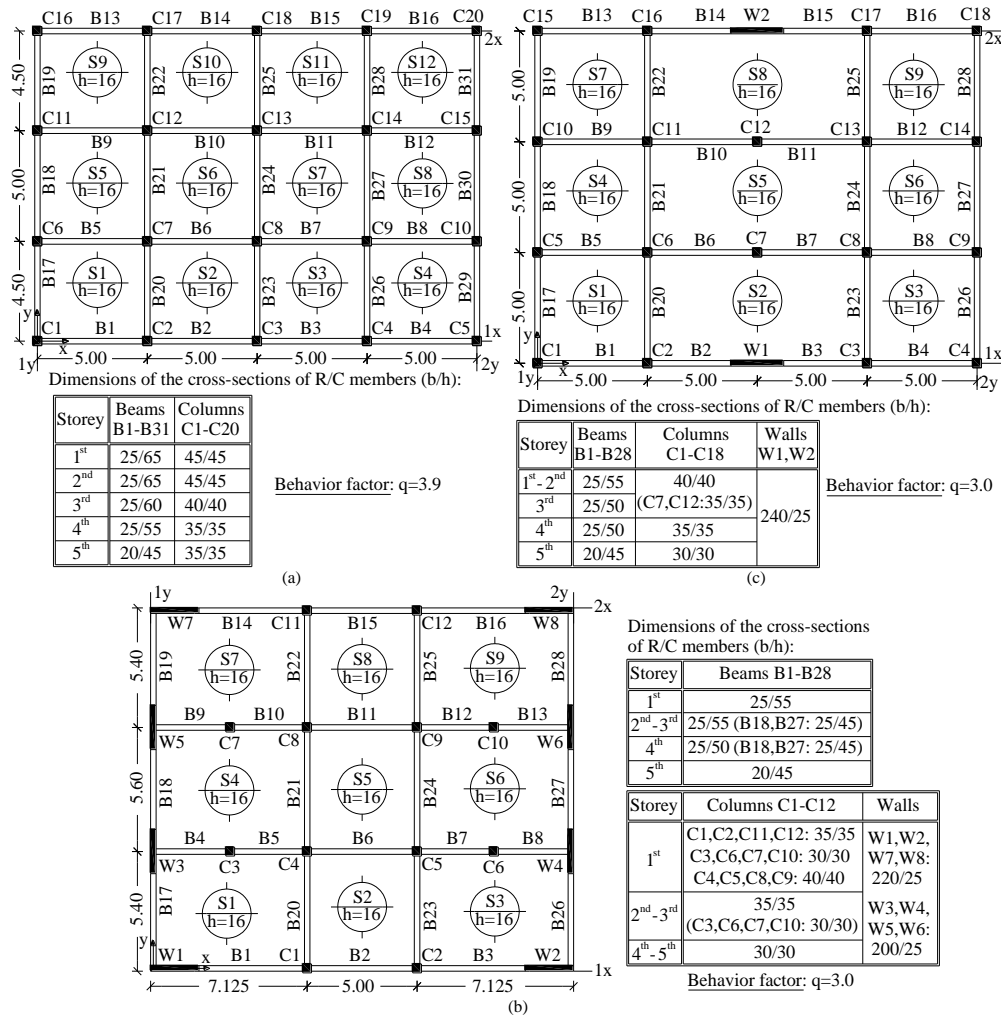


Fig. 1 Design parameters of the double-symmetric buildings SFxy (a), SWxy (b) and SWxFy (c)

repeated earthquakes, as well as the distance of the record from the fault.

2. Description, modeling and design of the selected buildings

2.1 Description of the buildings

For the purposes of the present investigation, three double-symmetric and three asymmetric in plan R/C buildings, with data supplied in Figs. 1 and 2 are studied. All buildings have five stories and structural system that consists of members in two perpendicular directions (axes x and y). More specifically, the following buildings are investigated (the classification follows the classification of structural types of the EN1998-1):

- Symmetric Frame System along both axes x and y SFxy: Double-symmetric building without walls (Fig. 1(a)).
- Symmetric Wall System along both axes x and y SWxy: Double-symmetric building with walls that take 80% of the base shear along both axes x and y (Fig. 1(b)).

- Symmetric Wall System along axis x and Frame System along axis y SWxFy: Double-symmetric building with walls that take more than 70% of the base shear along axis x , and without walls along axis y (Fig. 1(c)).
- Asymmetric Frame System along both axes x and y AFxy: Asymmetric in plan building without walls (Fig. 2(a)).
- Asymmetric Wall System along both axes x and y AWxy: Asymmetric in plan building with walls that take 67% of the base shear along axis x and 70% of the base shear along axis y (Fig. 2(b)).
- Asymmetric Frame System along axis x and Wall System along axis y AFxWy: Asymmetric in plan building with walls that take 70% of the base shear along axis y , and without walls along axis x (Fig. 2(c)).

All the above buildings are chosen as to represent a large amount of R/C buildings designed with the aid of modern seismic codes. It must also be noted that in order to investigate the influence of the structural eccentricity on the results, the choice of the asymmetric buildings is made bearing in mind that their structural systems must be corresponding to those of the double-symmetric ones. All

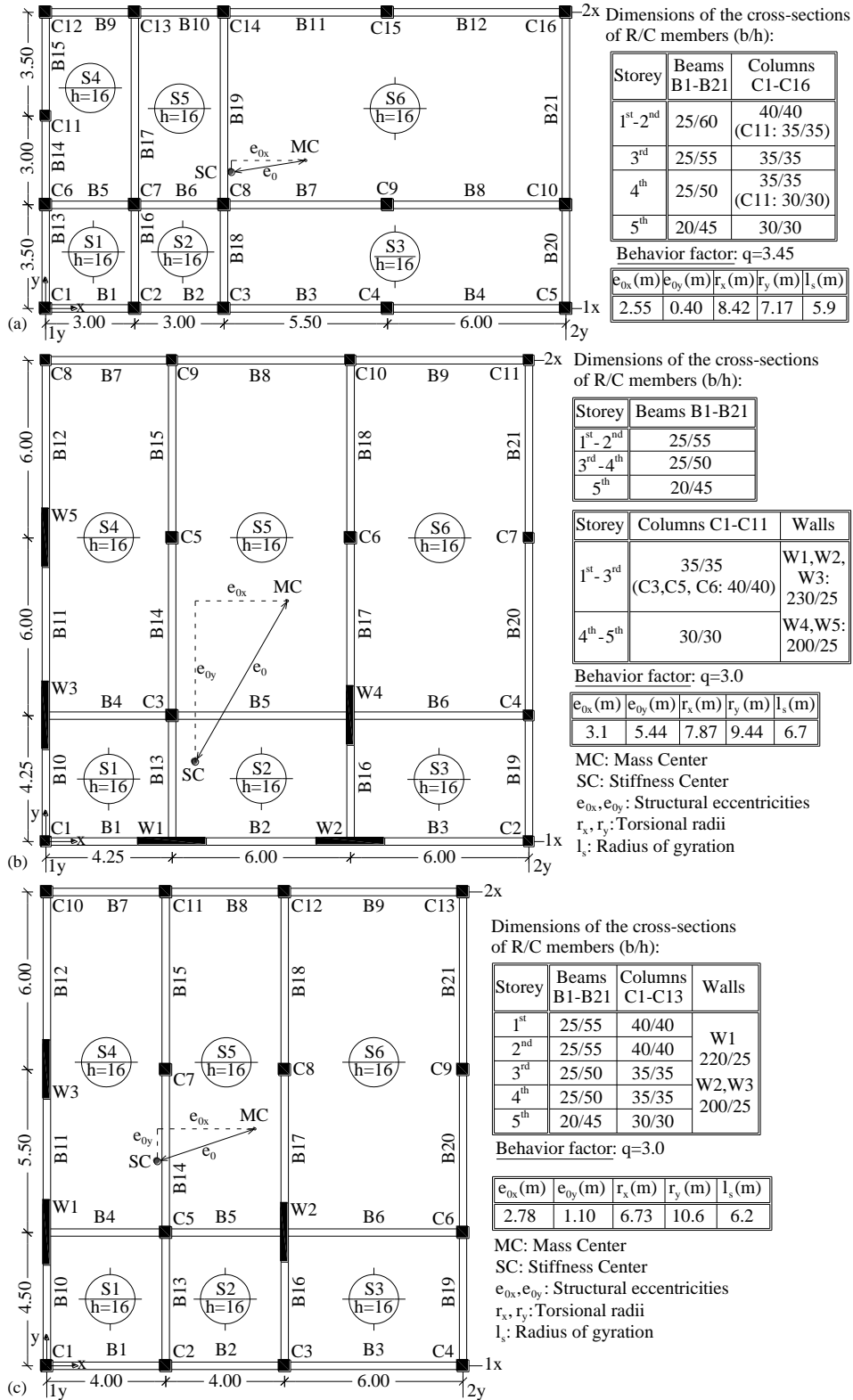


Fig. 2 Design parameters of the asymmetric buildings AFxy (a), AWxy (b) and AFxWy (c)

buildings are regular in elevation according to the criteria set by EN1998-1 (Paragraph 4.2.3.3). Also, for the asymmetric in plan buildings the distance between the mass centre and the stiffness centre, which defines the structural eccentricity e_0 , fulfils one of the following inequalities: $e_{0x} > 0.30r_x$ or $e_{0y} > 0.30r_y$. Therefore, these buildings display

a high degree of asymmetry and can be classified as irregular in plan buildings (EN1998-1, Paragraph 4.2.3.2). The three symmetric buildings are regular in plan. In Table 1 all the common design data of the examined buildings are presented.

Table 1 Common design data for all buildings

Stories' heights H_i	Ductility class	Concrete	Steel	Slab loads	Masonry loads	Design spectrum (EN1998-1)
3.2 m	Medium (DCM)	C20/25 $E_c=3 \cdot 10^7 \text{ kN/m}^2$ $\nu=0.2$ $w=25 \text{ kN/m}^3$	S500B $E_s=2 \cdot 10^8 \text{ kN/m}^2$ $\nu=0.3$ $w=78.5 \text{ kN/m}^3$	Dead: $G=1.0 \text{ kN/m}^2$ Live: $Q=2.0 \text{ kN/m}^2$	Perimetric beams: 3.6 kN/m^2 Internal beams: 2.1 kN/m^2	Reference PGA: $a_{gR}=0.24 \text{ g}$ Importance class: II $\rightarrow \gamma_I=1$ Ground type: C

Table 2 First 6 natural periods (sec) and corresponding modal participating mass ratios (%) of the symmetric buildings investigated

Mode	SFxy			SWxy			SWxFy		
	Period T	x-axis	y-axis	Period T	x-axis	y-axis	Period T	x-axis	y-axis
1	0.72	0	77	0.69	73	0	1.00	0	80
2	0.72	77	0	0.65	0	76	0.67	75	0
3	0.58	0	0	0.42	0	0	0.57	0	0
4	0.28	14	0	0.19	0	15	0.38	0	12
5	0.28	0	14	0.19	17	0	0.23	0	4
6	0.23	0	0	0.11	0	0	0.21	16	0

Table 3 First 6 natural periods (sec) and corresponding modal participating mass ratios (%) of the asymmetric buildings investigated

Mode	AFxy			AWxy			AFxWy		
	Period T	x-axis	y-axis	Period T	x-axis	y-axis	Period T	x-axis	y-axis
1	0.98	1	70	1.01	52	11	1.03	78	1
2	0.79	78	1	0.66	16	59	0.74	2	49
3	0.58	1	7	0.41	8	6	0.46	0	26
4	0.37	0	11	0.34	10	2	0.37	12	0
5	0.31	12	0	0.19	4	12	0.25	0	8
6	0.23	0	5	0.18	3	1	0.23	5	0

2.2 Elastic modeling and design of the structural members

For the buildings' modelling all basic recommendations of EN1998-1 (Paragraph 4.3.1), such as the diaphragmatic behaviour of the slabs, the rigid zones in the joint regions of beams/columns and beams/walls and the values of flexural and shear stiffness corresponding to cracked R/C elements are taken into consideration. For the modeling of the R/C walls the equivalent column model is used (Lew and Narov 1987). All buildings are considered to be fully fixed to the ground. Using the data given in Table 1, the upper limit values of the behaviour factor q according to EN1998-1 (Paragraph 5.2.2.2) are determined and are shown in Figs. 1 and 2. These values are used for the design of the examined buildings. Finally, the second-order effects have not been taken into consideration.

The buildings are analyzed for static vertical loads as well as for earthquake loads (taking into consideration the accidental torsion effects) using the modal response

spectrum analysis, as defined in EN1998-1. The R/C structural elements are designed following the provisions of EN1992-1-1 (2004) and EN1998-1 (2004). Consequently, a capacity design at frame joints is carried out only along the direction, where the buildings belong to the structural type of frame systems or frame-equivalent dual systems. It should also be noted that the choice of the dimensions of the structural elements' cross-sections as well as of their reinforcement is made bearing in mind the optimum exploitation of the structural materials strength (steel and concrete). Therefore, the Capacity Ratios CRs (where $CR = \text{Design value of Internal force} / \text{Design strength}$) of all the critical cross-sections due to bending and shear are close to 1.0. The professional program for R/C building analysis and design RAF (2014) is employed in both the analysis and design. The first 6 natural periods as well as the corresponding modal participating mass ratios of all models are given in Tables 2 and 3.

2.3 Modeling of the nonlinear behavior

For the modeling of the buildings' nonlinear behavior lumped plasticity (concentrated hinge) models at the column and beam ends as well as at the base of the walls, are used. The material inelasticity of the structural members is modeled by means of the Modified Takeda hysteresis rule (Otani 1974) (Fig. 3(a)), where the values of $\alpha=0.25$ and $\beta=0$ for the beams and $\alpha=0.50$ and $\beta=0$ for the vertical frame elements are used. It is important to notice that the effects of axial load-biaxial bending moments ($P-M_2-M_3$) interaction at column and wall hinges are taken into consideration by means of the $P-M_2-M_3$ interaction diagram shown in Fig. 3(b), which is implemented in the software used to conduct the analyses (Carr 2004). The yield moments as well as the parameters needed to determine the

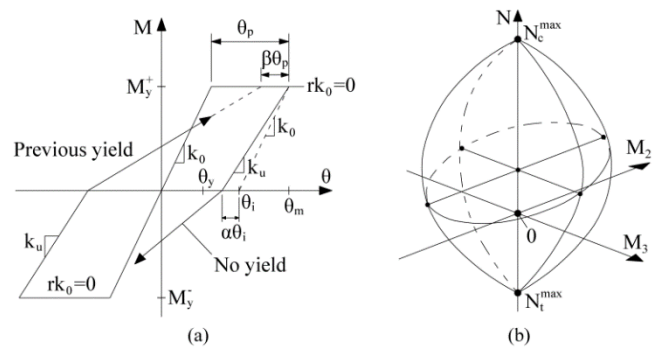


Fig. 3 Moment (M)-Rotation (θ) relationship (a) and P-M-M interaction diagram (b)

P-M₂-M₃ interaction diagram of the vertical elements' cross sections (Fig. 3(b)) are determined using appropriate software (XTRACT 2006). Moreover, structural damping has been modeled by using a Rayleigh damping matrix, such that the damping ratio is 5% for the first and second modes of vibration (Chopra 2001).

3. Seismic sequences

Because of the fact that the number of real seismic sequences is not sufficient in order to draw some useful conclusions, in the present study synthetic sequences that represent the ground motion features of real sequences are used. More specifically, the method introduced by Hatzigeorgiou and Beskos (2009) and based on the well-known Gutenberg-Richter law (Gutenberg and Richter 1954) is used. According to this method, random combinations of two or three real single earthquake records are selected in order to generate artificial seismic sequences. In particular, in this study four different cases of successive earthquakes are generated: (a) 20 double far-fault earthquakes, (b) 20 triple far-fault earthquakes, (c) 20 double near-fault earthquakes and (d) 20 triple near-fault earthquakes.

As mentioned above, in order to generate the seismic sequences, firstly an adequate number of real single earthquake records must be selected. For this reason, a suite of 40 pairs of horizontal bidirectional earthquake ground motions (20 far-fault and 20 near-fault records) is obtained from the PEER and the European strong motion database. In order to define whether a ground motion was recorded in the near- or far-field the commonly used distance to the fault is adopted. More specifically, far-fault ground motions are considered the records at more than 15 km from the fault trace, as the UBC (1997) suggests. Similarly, the near-fault motions were recorded at less than 15 km from the fault trace. At this point, it must be mentioned that there are also alternative criteria of distinguishing seismic motions into near- and far-fault records. Nevertheless, the above criterion is employed in the present paper, as it is one of the most common used criteria in relevant papers (e.g., Alavi and Krawinkler 2001, Iervolino and Cornell 2005, and Lopez *et al.* 2006). The seismic excitations, which are chosen from worldwide well known sites with strong seismic activity, were recorded on Soil Type C according to EN1998-1 and have magnitudes (M_s) between 5.5 and 7.8. The ground motion set employed is intended to cover a variety of conditions regarding tectonic environment and distance to fault rupture, thus representing a wide range of intensities and frequency content. The characteristics of the input ground motions are shown in Appendix A.

In order to generate double earthquake events, two randomly selected single real records are applied in sequence considering a gap of 100 sec (Hatzigeorgiou 2010a, b, Faisal *et al.* 2013) between the two successive earthquake records (foreshock-mainshock or mainshock-aftershock). This gap is considered adequate to cease the moving of the buildings due to damping. Moreover, as EN1998-1 suggests, the accelerograms of each one of the

two successive earthquake records are scaled to Peak Ground Acceleration $PGA = a_g \cdot S = 0.276 \text{ g}$, where a_g and S are the design ground acceleration and the soil factor respectively used for the elastic analysis of the buildings. Similarly, in order to generate triple earthquake events, three randomly selected single real records are applied in sequence considering a gap of 100 sec between the successive earthquake records (foreshock-mainshock-aftershock). In this case, appropriate scaling factors are applied to each one of the three single records in order to be scaled to the following PGA amplitude ratios: $0.853 \cdot 0.276 \text{ g}$ for the foreshock, 0.276 g for the mainshock and $0.853 \cdot 0.276 \text{ g}$ for the aftershock. Note that the above procedure of producing the double or triple earthquake records was applied separately for far- or near-fault records. For more information about the process followed to generate the seismic sequences the reader can consult Hatzigeorgiou and Beskos (2009), Hatzigeorgiou (2010a, b), and Faisal *et al.* (2013).

4. Nonlinear Time Response Analyses - Damage response parameters

The six buildings presented in paragraph 2.1 are analyzed by Nonlinear Time Response Analysis (NTRA) for each one of the 40 single ground motions and the 80 bidirectional seismic sequences (40 double and 40 triple earthquakes) taking into account the design vertical loads of the structures. The analyses are performed with the aid of the computer program Ruaumoko (Carr 2004). Furthermore, as the seismic incident angle with regard to structural axes is unknown, the two horizontal accelerograms of each ground motion are applied along horizontal orthogonal axes forming with the structural axes an angle $\theta=0^\circ, 30^\circ, 60^\circ, \dots, 330^\circ$. Thus, for each building and each pair of accelerograms 12 orientations were considered. As a consequence a total of 8640 NTHA (6 buildings \times (40+80) earthquake records \times 12 incident angles) were conducted in the present study. For each single ground motion as well as seismic sequence the damage state of the six buildings is determined. The seismic performance is expressed in the form of the **Interstorey Drift Ratio (IDR)**, as well as the **Maximum Interstorey Drift Ratio (MIDR)**. The MIDR, which is generally considered an effective indicator of global structural and nonstructural damage of R/C buildings (e.g., Gunturi and Shah 1992, Naeim 2011), has been used by many researchers for the assessment of the inelastic response of structures (e.g., Elenas and Meskouris 2001, Dimova and Negro 2005). It corresponds to the maximum drift among the four perimeter frames.

5. Results of the analytical investigation

In Fig. 4 the height-wise distribution of IDRs in case of the building AFxy subjected to the seismic sequence consisting of the far-fault earthquake records No4, No2 and

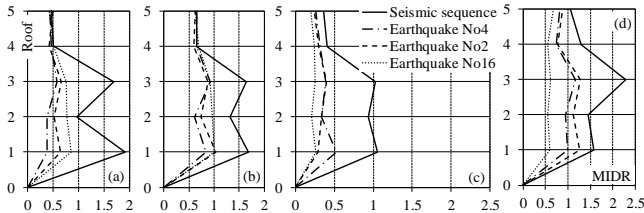


Fig. 4 Height-wise distribution of IDRs (%) in case of the building AFxy subjected to the far-fault successive earthquakes No4, No2 and No16. The diagrams present the IDRs for the 1x perimeter frame (a), the 2x perimeter frame (b), the 1y perimeter frame (c) and the 2y perimeter frame (d)

No16 (Appendix A) is indicatively presented. For comparison reasons the values of the IDRs caused by the individual seismic motions No4, No2 and No16 are also shown in the same figure. From this figure, we can see that the damage can be significantly higher in case of the seismic sequence compared to the damage induced by the individual ground motions.

Note that the value of IDR can be up to 2.8 times larger (IDR 1y of the 2nd floor, Fig. 4(c)) in case of the successive earthquakes than its value when the building is subjected to individual ground motions. Moreover, it is obvious that the influence of the seismic sequence on the IDR depends on the storey and the frame along which the IDR is computed. We notice, for example that the 4th and 5th floor IDRs of frames along axis x attain almost the same values for the seismic sequence and the individual ground motions (Figs. 4(a) and 4(b)).

In order to generalize trends, the Index of Influence of Seismic Sequence (IISS) for every seismic sequence is introduced

$$IISS = \frac{MIDR_{ss} - \max(MIDR_1, MIDR_2, MIDR_3)}{\max(MIDR_1, MIDR_2, MIDR_3)} \cdot 100 (\%) \quad (1)$$

where $MIDR_{ss}$: the MIDR of the building subjected to the seismic sequence; $MIDR_1$ the MIDR of the building subjected to the 1st earthquake of the seismic sequence, $MIDR_2$ the MIDR of the building subjected to the 2nd earthquake of the seismic sequence, $MIDR_3$ the MIDR of the building subjected to the 3rd earthquake of the seismic sequence (in case of triple earthquakes).

Figs. 5 and 6 illustrate the maximum, the mean and the minimum values of IISS over all the seismic sequences in case of double or triple earthquakes respectively. It must be mentioned that the values of IISS have been computed separately for the near- and far-fault earthquake records. Moreover, the values of IISS presented in Figs. 5 and 6 were computed taking into account both the incident angles $\theta=0^\circ$ and $\theta=90^\circ$ ($MIDR_i = \max\{MIDR_i(\theta=0^\circ); MIDR_i(\theta=90^\circ)\}$, $i=1,2,3,ss$). Note that the mean values of the IISS quantify the general trends regarding the damage caused by the successive earthquakes compared to the damage induced by the individual seismic motions. On the other hand, the maximum and the minimum values of the IISS reflect the bandwidth of the interval where the IISS fluctuates.

The influence of successive earthquake phenomena on

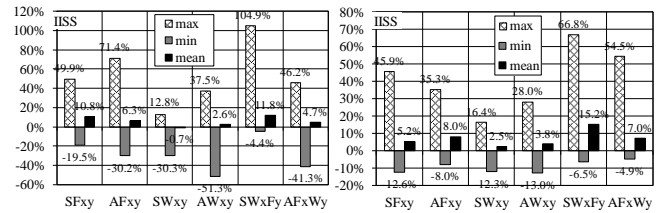


Fig. 5 Maximum, mean and minimum values of IISS in case of seismic sequences consisting of two far-fault (a) or near-fault (b) earthquakes

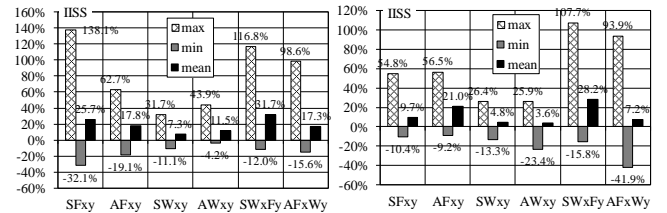


Fig. 6 Maximum, mean and minimum values of IISS in case of seismic sequences consisting of three far-fault (a) or near-fault (b) earthquakes

the seismic damage can be strong depending on the special characteristics of the structure, the number of the successive earthquakes, as well as the distance of the record from the fault. The analyses revealed that, as it was expected, for the vast majority of the seismic sequences, the structural damage is larger when the buildings are subjected to successive earthquakes compared to corresponding single seismic events. This conclusion is reflected to the fact that, as shown in Figs. 5 and 6, with the exception of the building SWxy subjected to double far-fault seismic motions (for this case $IISS=-0.7\%$), the mean IISS attains positive values. Note that the mean IISS can reach the value of 31.7% for the building SWxFy subjected to triple far-fault earthquakes (Fig. 6(a)).

Of significant importance is the fact that there are certain seismic sequences where the damage caused by the successive earthquakes is notably higher than the damage induced by the individual seismic motions. Note that the maximum IISS can reach the value of 104.9% in case of seismic sequences consisting of two earthquakes (building SWxFy, Fig. 5(a)) and the value of 138.1% in case of seismic sequences consisting of three earthquakes (building SFxy, Fig. 6(a)). However, there are also a small number of seismic sequences, where the structural damage caused by the sequential earthquakes is smaller than the damage caused by the single ground motions. This is expressed with the aid of the negative values that attains the minimum IISS. We can see that the minimum IISS can reach the value of -51.3% in case of seismic sequences consisting of two earthquakes (building AWxy, Fig. 5(a)) and the value of -41.9% in case of seismic sequences consisting of three earthquakes (building AFxWy, Fig. 6(b)). The above observation can be attributed to the fact that, in case of certain buildings and seismic sequences, the first earthquake can significantly alter the dynamic and structural

characteristics of the building (e.g., increase of the structure's fundamental period) in such a way that during the second (and the third) earthquake the seismic forces will be lower than the case where every earthquake of the sequence acts separately.

As aforementioned, the effects of successive earthquakes on the seismic damage depend on the special structural characteristics of the building. From the Figs. 5 and 6 it is obvious that the values of IISS (maximum and mean) are smaller for the wall systems SWxy and AWxy. We notice that, for these buildings, the mean IISS does not exceed the value of 11.5% (triple far-fault earthquakes, Fig. 6(a)). This conclusion could be explained in the following way: The buildings SWxy and AWxy have r/c walls along axes x and y . As was presented in paragraph 2.1, these walls take approximately 70% of the seismic forces along both axes x and y . Given that the aforementioned walls are designed to receive the seismic shear forces maintaining an elastic behavior (with the possible exception of their critical region (EN1998-1, Paragraph 5.4.1.2.3) which is designed on the basis of the capacity design rules), the specific buildings have a vertical seismic resistant part that takes by far the largest portion of seismic forces while remaining almost elastic. As a result, the buildings SWxy and AWxy preserve a relatively stable seismic resistant behavior during the seismic sequence. On the contrary, the largest values of IISS appear for the building SWxFy. In this case, the mean IISS can attain the value of 31.7% for the seismic sequences consisting of three far-fault earthquakes (Fig. 6(a)).

Moreover, the impact of the seismic sequences on the structural damage is affected by the distance of the record from the fault. However, no certain trend can be observed, since it depends on the building and on the number of the successive earthquakes. Concerning the double earthquakes, it can be seen that, with the exception of the building SFxy, the mean IISS is larger for the near-fault ground motions. On the contrary, we can see that regarding the triple earthquake records, with the exception of the buildings AFxy and AFxWy, the mean IISS is larger for the far-fault earthquakes. Note for example that the mean IISS for the building SFxy attains the values of 25.7% and 9.7% in case of far-fault and near-fault seismic motions respectively (Fig. 6). As far as the maximum IISS is concerned, we notice that for the most buildings it attains larger values for the far-fault seismic records. As an example we can notice that the maximum IISS for the building SWxFy attains the values of 104.9% and 66.8% in case of far-fault and near-fault seismic motions respectively (Fig. 5).

In order to examine the effect that the number of sequential earthquakes has on the damage response of the investigated buildings, the maximum, the mean and the minimum values of IISS over all the double (Fig. 7(a)) and the triple (Fig. 7(b)) earthquakes were computed. Note that for the determination of these values of IISS, both the near- and the far-fault earthquake records were used. Moreover, the values of IISS presented in Fig. 7 were computed taking into account both the incident angles $\theta=0^\circ$ and $\theta=90^\circ$ ($MIDR_i = \max\{MIDR_i(\theta=0); MIDR_i(\theta=90)\}$, $i=1,2,3,ss$). From Fig. 7 it is obvious that, as was expected, the mean and the maximum value of IISS are larger in case of the

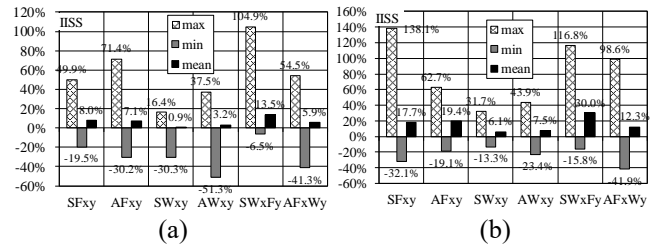


Fig. 7 Maximum, mean and minimum values of IISS in case of seismic sequences consisting of two (a) and three (b) earthquakes

seismic sequences consisting of three ground motions. This conclusion, which can be attributed to the fact that in case of three successive earthquakes the cumulative structural damage is larger than the damage caused by double seismic ground motions, is valid for all the buildings investigated in the present study. We can notice that the mean IISS ranges between 0.9% and 13.5% for the double earthquake motions (Fig. 7(a)) and between 6.1% and 30.0% for the triple earthquake records (Fig. 7(b)). Similarly, the maximum IISS ranges between 16.4% and 104.9% for the double earthquake motions (Fig. 7(a)) and between 31.7% and 138.1% for the triple earthquake records (Fig. 7(b)).

The influence of the incident angle on the 1st storey IDRs of buildings AFxWy and SWxy subjected to seismic sequences consisting of far-fault earthquake records is presented in Fig. 8. From this figure, we can see that the impact of the successive earthquakes on the IDR strongly depends on the orientation of the seismic motion. This observation can be attributed to the fact that rotating the seismic records to another orientation can significantly alter the pattern of the induced seismic forces of both the individual and the sequential ground motions. Notice, for example that in case of building AFxWy (Fig. 8(a)) the IDR caused by the seismic sequence consisting of the earthquakes No6 and No19 for incident angle $\theta=120^\circ$ is almost two times larger than the IDR caused by the corresponding individual ground motions. However, for incident angles $\theta=0^\circ$, and $\theta=180^\circ$, the IDR caused by the seismic sequence attains the same values as the one produced by the individual earthquake No6. Similarly, in case of building SWxy (Fig. 8(b)) the IDR caused by the seismic sequence consisting of the earthquakes No4, No2 and No16 for incident angles $\theta=30^\circ$, 60° , 120° , 240° and 270° is more than two times larger than the IDR caused by the individual ground motions. However, for incident angle $\theta=180^\circ$, the IDR caused by the seismic sequence attains almost the same value as the one produced by the individual earthquake No16.

Figs. 9 and 10 illustrate the variation of the maximum, the mean and the minimum values of IISS with the incident angle of the ground motion. From these figures we can see that the influence of the successive earthquakes on the damage depends on the orientation of the seismic motion. The incident angle can radically alter the values of IISS depending on the special characteristics of the structure, the number of the successive earthquakes, as well as the distance of the record from the fault. Note that the mean and

maximum IISS can reach the values of 164.5% (building SWxy under triple near-fault earthquakes for incident angle $\theta=330^\circ$, Fig. 9(b)) and 187.2% (building SWxy under triple far-fault earthquakes for incident angle $\theta=150^\circ$, Fig. 9(b)) respectively.

Figs. 9 and 10 show that the influence of the incident angle is larger for the maximum values of IISS and much smaller for the mean values. This was expected, since the use of the mean IISS normalizes the peaks corresponding to individual seismic sequences. As an example, we can see that in case of the building SWxy subjected to seismic sequences consisting of three far-fault earthquakes the maximum IISS for incident angle $\theta=150^\circ$ is almost 7 times larger than the corresponding value for incident angle $\theta=330^\circ$ (Fig. 9(b)). Similarly, in case of the building AWxy subjected to double near-fault earthquake records the maximum IISS for incident angle $\theta=210^\circ$ is almost 15 times larger than the corresponding value for incident angle $\theta=90^\circ$ (Fig. 10(a)). Another significant observation made from the above figures is that, as was expected, for the vast majority of the incident angles the values of maximum and mean IISS are larger for the seismic sequences consisting of three earthquakes compared to the values produced for the double earthquakes.

Regarding the minimum IISS, from Figs. 9, 10 we can see that it attains negative values for all the incident angles, which means that there are cases of seismic sequences where the damage induced by the successive earthquakes is smaller than the damage caused by the corresponding single seismic events. Notice for example that the minimum IISS for the building SWxy under double far-fault earthquakes ranges between -7.5% for incident angle $\theta=300^\circ$ and -82.0% for incident angle $\theta=30^\circ$ (Fig. 9(a)).

6. Conclusions

The present paper examines the effect of seismic sequences on the damage response of 3D multistorey buildings with various structural systems. More specifically, six 3D, medium-rise R/C buildings are studied. The buildings are analyzed by means of Nonlinear Time Response Analysis for 40 single ground motions as well as for 80 bidirectional seismic sequences. Furthermore, in order to account for the influence of the incident angle on

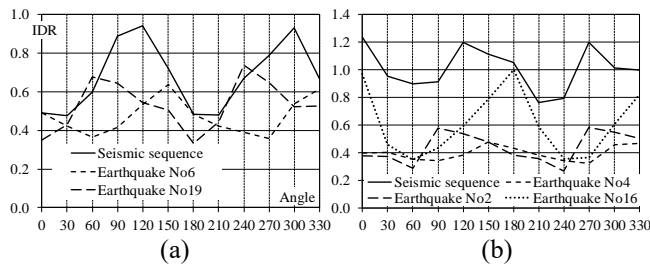


Fig. 8 1st storey IDRs along x-axis of individual earthquakes as well as seismic sequences in case of (a) building AFxWy under successive far-fault earthquakes No6 and No19 and (b) building SWxy under successive far-fault earthquakes No4, No2 and No16

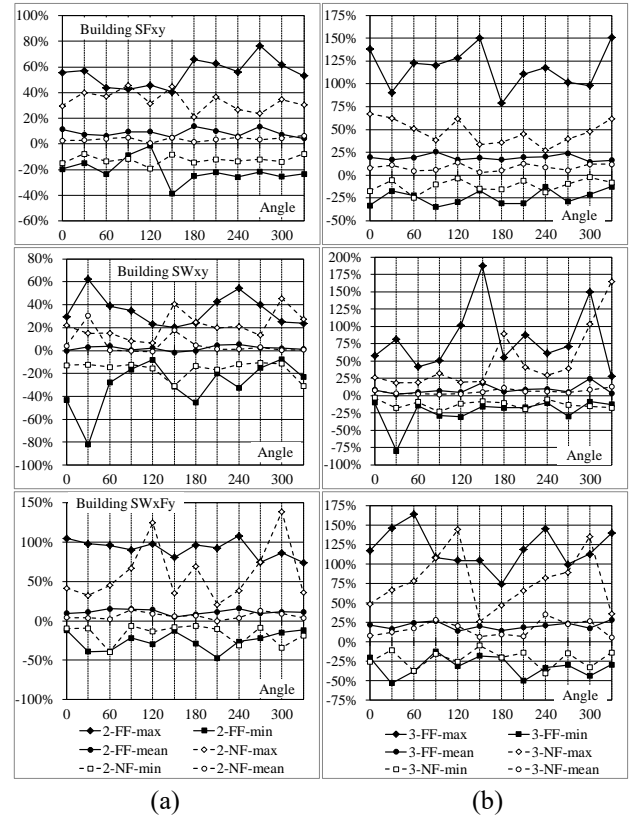


Fig. 9 Variation of maximum, mean and minimum values of IISS with the incident angle in case of symmetric buildings subjected to seismic sequences consisting of two (a) and three (b) earthquakes

the structural response, the two horizontal accelerograms of each ground motion are applied along horizontal orthogonal axes forming an angle $\theta=0^\circ, 30^\circ, 60^\circ, \dots, \dots, 330^\circ$ with the structural axes. For the evaluation of the expected structural damage state of each building the maximum interstorey drift ratio is determined. The comparative assessment of the results leads to the following conclusions:

- For the vast majority of the seismic sequences, successive ground motions lead to increase of the structural damage compared to the damage caused by the corresponding single seismic events. The difference between single and successive earthquakes can reach the value of 187.2%. Thus, the successive earthquake phenomenon cannot be ignored and should be taken into account for the seismic design, as well as for the seismic demand assessment of the structures.
- The effect of the successive earthquake phenomenon on the seismic damage is stronger for seismic sequences consisting of three ground motions compared to the case of double seismic events.
- The influence of the successive earthquakes on the structural damage is smaller for the wall systems SWxy and AWxy. On the contrary, it is more obvious for the building SWxFy.
- The impact of the seismic sequences on the structural damage is affected by the distance of the record from the fault. However, no certain trend can be observed,

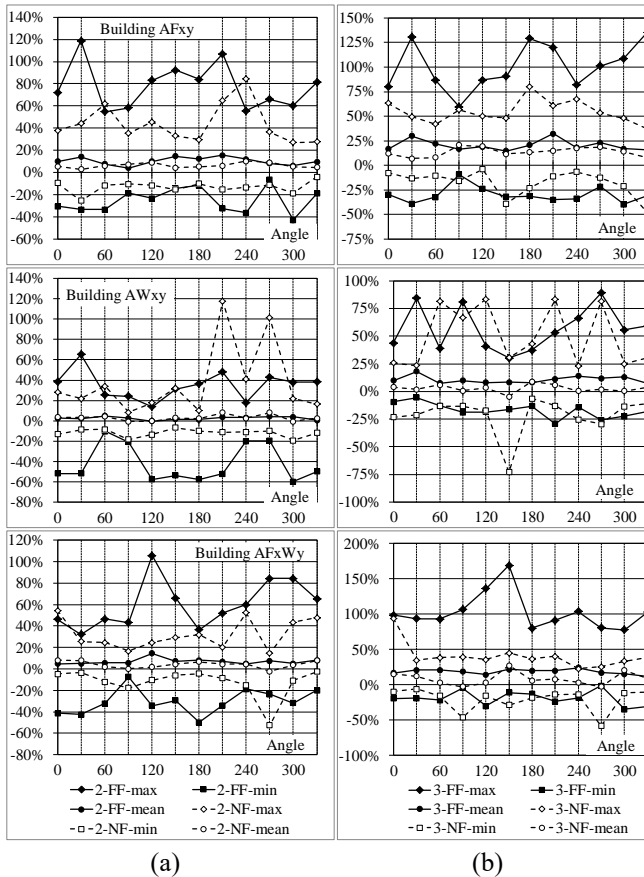


Fig. 10 Variation of maximum, mean and minimum values of IISS with the incident angle in case of asymmetric buildings subjected to seismic sequences consisting of two (a) and three (b) earthquakes

since it depends on the building and on the number of the sequential earthquakes.

- The incident angle strongly influences the successive earthquake phenomenon depending on the special characteristics of the structure, the number of the successive earthquakes, as well as the distance of the record from the fault.

It must be noted that the aforementioned conclusions are valid for the buildings investigated in the present study. However, they provide a good insight into the impact of sequential earthquakes on the seismic damage of 3D, medium-rise, R/C buildings subjected to bidirectional earthquake records.

References

- Alavi, B. and Krawinkler, H. (2001), "Effects of near-fault ground motions on frame structures", Blume center report #138. Stanford (CA), 301p.
- Amadio, C., Fragiaco, M. and Rajgelj, S. (2003), "The effects of repeated earthquake ground motions on the non-linear response of SDOF systems", *Earthq. Eng. Struct. Dyn.*, **32**(2), 291-308.
- ASCE/SEI 41-06 (2008), *Seismic Rehabilitation of Existing Buildings*, ASCE.
- Athanatopoulou, A.M. (2005), "Critical orientation of three correlated seismic components", *Eng. Struct.*, **27**(2), 301-312.
- Athanatopoulou, A.M., Tsourekas, A. and Papamanolis, G. (2005), "Variation of response with incident angle under two horizontal correlated seismic components", *Proceedings of Earthquake Resistant Engineering Structures V*, Skiathos, Greece, May.
- Augenti, N. and Parisi, F. (2010), "Learning from construction failures due to the 2009 L'Aquila, Italy, earthquake", *J. Struct. Eng.*, ASCE, **24**(6), 536-555.
- Carr, A.J. (2004), *Ruaumoko-A Program for Inelastic Time-History Analysis: Program Manual*, Department of Civil Engineering, University of Canterbury, New Zealand.
- Chopra, A.K. (2001), *Dynamics of Structures: Theory and Applications to Earthquake Engineering*, (2nd Edition), Prentice-Hall: Englewood Cliffs, NJ, USA.
- Dimova, S.L. and Negro, P. (2005), "Seismic assessment of an industrial frame structure designed according to Eurocodes. Part 2: Capacity and vulnerability", *Eng. Struct.*, **27**(5), 724-735.
- Efraimiadou, S., Hatzigeorgiou, G.D. and Beskos, D.E. (2013), "Structural pounding between adjacent buildings subjected to strong ground motions. Part II: The effect of multiple earthquakes", *Earthq. Eng. Struct. Dyn.*, **42**(10), 1529-1545.
- Elenas, A. and Meskouris, K. (2001), "Correlation study between seismic acceleration parameters and damage indices of structure", *Eng. Struct.*, **23**(6), 698-704.
- Elnashai, A.S., Jefferson, T., Fiedrich, F., Cleveland, L.J. and Gress T. (2009), Impact of New Madrid seismic zone earthquakes on the central USA: Volume I. Mid-America Earthquake (MAE) Center report, no.09-03.
- EN1992-1-1 (2004), Eurocode 2, *Design of Concrete Structures, Part 1-1: General rules and rules for buildings*, European Committee for Standardization, Brussels.
- EN1998-1 (2004), Eurocode 8, *Design of structures for earthquake resistance - Part 1: General rules, seismic actions and rules for buildings*, European Committee for Standardization, Brussels.
- Faisal, A., Majid, T.A. and Hatzigeorgiou, G.D. (2013), "Investigation of story ductility demands of inelastic concrete frames subjected to repeated earthquakes", *Soil Dyn. Earthq. Eng.*, **44**, 42-53.
- FEMA-356 (2000), *Prestandard and Commentary for the Seismic Rehabilitation of Buildings*, Federal Emergency Management Agency, Washington DC.
- Fontara, I.K.M., Kostinakis, K.G., Manoukas, G.E. and Athanatopoulou, A.M. (2015), "Parameters affecting the seismic response of buildings under bi-directional excitation", *Struct. Eng. Mech.*, **53**(5), 957-979.
- Frangiaco, M., Amadio, C. and Macorini, L. (2004), "Seismic response of steel frames under repeated earthquake ground motions", *Eng. Struct.*, **26**(13), 2021-2035.
- Gunturi, S.K.V. and Shah, H.C. (1992), "Building specific damage estimation", *Proceedings of 10th World Conference on Earthquake Engineering*, Madrid, Spain, July.
- Gutenberg, B. and Richter, C.F. (1954), *Seismicity of the Earth and Associated Phenomena*, (2nd Edition), Princeton University Press, Princeton NJ, USA.
- Hatzigeorgiou, G.D. and Beskos, D.E. (2009), "Inelastic displacement ratios for SDOF structures subjected to repeated earthquakes", *Eng. Struct.*, **31**(11), 2744-2755.
- Hatzigeorgiou, G.D. (2010a), "Behavior factors for nonlinear structures subjected to multiple near-fault earthquakes", *Comput. Struct.*, **88**(5), 309-321.
- Hatzigeorgiou, G.D. and Liolios, A.A. (2010), "Nonlinear behaviour of RC frames under repeated strong ground motions", *Soil Dyn. Earthq. Eng.*, **30**(10), 1010-1025.
- Hatzigeorgiou, G.D. (2010b), "Ductility demand spectra for multiple near- and far-fault earthquakes", *Soil Dyn. Earthq.*

- Eng., **30**(4), 170-183.
- Iervolino, I. and Cornell, C.A. (2005), "Record selection for seismic analysis of structures", *Earthq. Spectra*, **21**(3), 685-713.
- Jing, L.P., Liang, H.A., Li, Y.Q. and Liu, C.H. (2011), "Characteristics and factors that influenced damage to dams in the Ms 8.0 Wenchuan earthquake", *Earthq. Eng. Eng. Vib.*, **10**(3), 349-358.
- Kalkan, E. and Kunnath, S.K. (2006), "Effects of fling step and forward directivity on seismic response of buildings", *Earthq. Spectra*, **22**(2), 367-390.
- Kostinakis, K.G., Athanatopoulou, A.M. and Avramidis, I.E. (2010), "Influence of orientation of recorded ground motion components on the reinforcing steel area in concrete frame elements", *Proceedings of 9th US National and 10th Canadian Conference on Earthquake Engineering*, Toronto, Canada, July.
- Kostinakis, K.G., Athanatopoulou, A.M. and Avramidis, I.E. (2012), "Orientation effects of horizontal seismic components on longitudinal reinforcement in R/C Frame elements", *Nat. Haz. Earth Syst.*, **12**(1), 1-10.
- Kostinakis, K.G., Athanatopoulou, A.M. and Avramidis, I.E. (2013), "Evaluation of inelastic response of 3D single-story R/C frames under bi-directional excitation using different orientation schemes", *Bull. Earthq. Eng.*, **11**(2), 637-661.
- Lagaros, N.D. (2010), "Multicomponent incremental dynamic analysis considering variable incident angle", *Struct. Infrastruct. Eng.*, **6**(1-2), 77-94.
- Lew, I.P. and Narov, F. (1987), "Three dimensional equivalent frame analysis of shear walls", *Concrete Int. Des. Constr.*, **5**(10), 25-30.
- Lopez, O.A., Hernandez, J.J., Bonilla, R. and Fernandez, A. (2006), "Response spectra for multicomponent structural analysis", *Earthq. Spectra*, **22**(1), 85-113.
- Lucchini, A., Monti, G. and Kunnath, S. (2011), "Nonlinear response of two-way asymmetric single-story building under biaxial excitation", *J. Struct. Eng.*, ASCE, **137**(1), 34-40.
- Naeim, F. (2011), *The Seismic Design Handbook*, (2nd Edition), Kluwer Academic, Boston, USA.
- NEHRP (2003), *Recommended provisions for seismic regulations for new buildings and other Structures*, FEMA450, Building Seismic Safety Council, Washington DC.
- Otani, A. (1974), "Inelastic analysis of RC frame structures", *J. Struct. Div.*, ASCE, **100**(7), 1433-1449.
- Pacific Earthquake Engineering Research Centre (PEER): Strong Motion Database. <http://peer.berkeley.edu/smcat/>
- Priestley, M.J.N. (1988), "The Whittier Narrows, California earthquake of October 1, 1987- damage to the I-5/I-605 separator", *Earthq. Spectra*, **4**(2), 389-405.
- RAF Ver. 4.4: Structural Analysis / Design Software (2014), TOL-Eng. Soft. House, Iraklion, Crete, Greece.
- Rigato, A.B. and Medina, R.A. (2007), "Influence of angle of incidence on seismic demands for inelastic single-storey structures subjected to bi-directional ground motions", *Eng. Struct.*, **29**(10), 2593-2601.
- Ruiz-Garcia, J. and Negrete-Manriquez, J.C. (2011), "Evaluation of drift demand in existing steel frames under as-recorded far-field and near-field mainshock-aftershock seismic sequences", *Eng. Struct.*, **33**(2), 621-634.
- Ruiz-Garcia, J., Martin, M.V. and Teran-Gilmore, A. (2014), "Effect of seismic sequences in reinforced concrete frame buildings located in soft-soil sites", *Soil Dyn. Earthq. Eng.*, **63**, 56-68.
- Sarno, L.D. (2013), "Effects of multiple earthquakes on inelastic structural response", *Eng. Struct.*, **56**, 673-681.
- Shin, J., Kim, J. and Lee, K. (2014), "Seismic assessment of damaged piloti-type RC building subjected to successive earthquakes", *Earthq. Eng. Struct. Dyn.*, **43**(11), 1603-1619.
- The European Strong-Motion Database. http://www.isesd.hi.is/ESD_Local/frameset.htm
- UBC (1997), *Structural Engineering Design Provisions. Uniform Building Code*, International Conference of Building Officials, Vol. 2, Whittier, CA, USA.
- XTRACT Ver. 3.0.5: Cross-sectional Structural Analysis of Components (2006), Imbsen Software Systems, Sacramento, CA, USA.
- Zahid, M.Z.A.M., Majid, T.A. and Faisal, A. (2012), "Effect of repeated near field earthquake to the high-rise Rc building", *Aust. J. Basic Appl. Sci.*, **6**(10), 129-138.
- Zhai, C-H., Wen, W-P., Chen, Z., Li, S. and Xie, L.L. (2013), "Damage spectra for the mainshock-aftershock sequence-type ground motions", *Soil Dyn. Earthq. Eng.*, **45**, 1-12.

SA

Appendix A

Table A1 Far-fault ground motions recorded on Soil Type C according to EN1998-1

No	Date	Earthquake name	Magnitude (Ms)	Closest distance (Km)	Component (deg)	PGA (g)
1	15/10/1979	Imperial Valley	6.9	28.7	012/282	0.270/0.254
2	28/06/1992	Landers	7.4	69.5	000/090	0.081/0.097
3	24/04/1984	Morgan Hill	6.1	32.5	001/271	0.071/0.071
4	01/10/1987	Whittier Narrows	5.7	28.1	090/180	0.042/0.059
5	17/01/1994	Northridge	6.7	71.1	000/090	0.072/0.066
6	02/05/1983	Coalinga	6.5	47.3	270/360	0.147/0.131
7	15/04/1979	Montenegro	6.9	96	E-W/N-S	0.055/0.040
8	25/02/1981	Aktion (Greece)	6.3	19	030/120	0.117/0.120
9	23/03/1983	Kefallinia (Greece)	6.2	72	E-W/N-S	0.025/0.022
10	07/12/1988	Spitak	6.7	36	E-W/N-S	0.183/0.183
11	20/06/1990	Manjil (Iran)	7.4	61	N40E/N50W	0.097/0.086
12	26/09/1997	Umbria Marche (It)	6	21	N-S/W-E	0.117/0.109
13	17/08/1999	Izmit (Turkey)	7.6	29	W-E/S-N	0.129/0.091
14	12/11/1999	Duzce (Turkey)	7.2	113	S-N/E-W	0.022/0.021
15	15/06/1995	Aigion (Greece)	6.5	92	261/351	0.051/0.057
16	28/06/1992	Landers	7.4	24.9	270/360	0.245/0.152
17	17/01/1994	Northridge	6.7	36.9	090/180	0.290/0.264
18	09/02/1971	San Fernando	6.6	21.2	090/180	0.210/0.174
19	24/11/1987	Superstition Hills	6.6	28.3	225/315	0.180/0.247
20	24/01/1980	Livermore	5.5	17.6	180/270	0.154/0.076

Table A2 Near-fault ground motions recorded on Soil Type C according to EN1998-1

No	Date	Earthquake name	Magnitude (Ms)	Closest distance (Km)	Component (deg)	PGA (g)
1	17/01/1994	Northridge	6.7	6.4	090/360	0.604/0.843
2	17/01/1994	Northridge	6.7	12.3	000/090	0.303/0.443
3	01/10/1987	Whittier Narrows	5.7	9.8	207/297	0.219/0.212
4	19/05/1940	Imperial Valley	7.2	8.3	180/270	0.313/0.215
5	28/06/1966	Parkfield	6.1 (M)	9.2	050/320	0.246/0.273
6	25/04/1992	Cape Mendocino	7.1	9.5	000/090	0.590/0.662
7	13/03/1992	Erzincan (Turkey)	6.9 (M)	2.0	N-S/E-W	0.515/0.496
8	18/10/1989	Loma Prieta	7.1	14.5	000/090	0.529/0.443
9	11/09/1976	Friuli (Italy)	5.5	7	E-W/N-S	0.105/0.230
10	04/07/1978	Volvi (Greece)		15	E-W/N-S	0.099/0.115
11	24/02/1981	Aktion (Greece)	6.6	10	N30/N120	0.230/0.310
12	07/12/1988	Spitak		10	E-W/N-S	0.103/0.147
13	26/09/1997	Umbria Marche (It)	6	5	N-S/W-E	0.199/0.223
14	12/11/1999	Duzce (Turkey)	7.2	0	W-E/S-N	0.513/0.377
15	15/10/1979	Imperial Valley	6.9	8.5	045/315	0.327/0.260
16	17/08/1999	Kocaeli (Turkey)	7.8	2.6	060/330	0.268/0.349
17	27/01/1980	Livermore	5.5	3.6	270/360	0.258/0.233
18	24/11/1987	Superstition Hills	6.6	13.9	000/090	0.358/0.258
19	24/04/1984	Morgan Hill	6.1	3.4	150/240	0.156/0.312
20	24/04/1984	Morgan Hill	6.1	12.8	270/360	0.224/0.348